Flow maps and flow patterns of R1233zd(E) in a circular minichannel at low, medium and high values of saturation pressure

Stanisław Głuch[a], Michał Pysz[b], Dariusz Mikielewicz[c]

[a] Gdańsk University of Technology, Gdańsk, Poland stanislaw.gluch@pg.edu.pl
[b] Gdańsk University of Technology Gdańsk, Poland michal.pysz@pg.edu.pl
[c] Gdańsk University of Technology Gdańsk, Poland dariusz.mikielewicz@pg.edu.pl

Abstract:

There is a gap in knowledge regarding the flow pattern of low-boiling working fluids in the range of high saturation temperatures (above 120°C) and medium and high reduced pressures (0.5-0.9). Data are present in the literature for similar values of reduced pressures, but for lower values of saturation temperature. This is due to the existing refrigeration applications of these working fluids. At high values of reduced pressure, the density of the gas phase is relatively high, and the density of the liquid phase is low. There is a low specific volume difference between the liquid and gas phases. The liquid phase has a low surface tension value. The gas phase has a relatively high viscosity, and the liquid phase has a reduced value of viscosity. These changes in the parameters of refrigerants cause significant differences in flow structures. At a low value of reduced pressure, 0.2, the occurrence of annular flow was observed already at a quality of 0.07 for a mass velocity of G=355 [kg/(m^2·s)], while for a reduced pressure of 0.8, annular flow occurs much later, at a quality of 0.47 for the same mass velocity. Mass velocity flow maps in a function of quality for constant values of reduced pressure and flow maps for reduced pressure as a function of quality at constant mass velocity are presented. Flow maps are compared with correlations for transition lines between intermittent and annular flow structures from literature. Authors new correlation for transition line for researched conditions is presented. New prediction method is the only one which managed to predict transition to annular flow at high values of reduced pressure for collected experimental data.

Keywords:

two-phase flow; flow patterns; flow maps; R1233zd(E); high value of reduced pressure; annular flow transition line prediction

1. Introduction

An important trend in the development of new technologies is the miniaturization of technical objects. This effort requires extensive basic knowledge of fluid mechanics and heat transfer in single-phase convection and boiling and condensation in flow. The ability to accurately predict pressure drops and heat transfer, as well as the selection of geometry and operating conditions, are important factors in the design and selection of optimal heat exchanger settings. There is now a growing interest in low global warming potential (GWP) refrigerants. New European regulations require that air conditioning and refrigeration applications cannot be manufactured using fluorinated greenhouse gases with a GWP greater than 150 (EU directive 2019/1937). This leads to the use of new, environmentally friendly agents such as CO2, which operates in the near-critical and supercritical areas. Other applications, such as high-temperature heat pumps or ORC cycles, operate at much higher parameters than refrigeration systems. In 2022 energy price crisis resulted in immense demand for industrial high temperature heat pumps. Data available in the literature on heat transfer by refrigerants at high saturation temperatures are scarce. Studies of structures and flow maps are even more scarce. Many heat transfer correlations such as [1,2]created for specific flow pattern. It is essential to predict flow pattern to accurately calculate heat transfer coefficient.

1.1. Previous research on flow pattern maps

Cheng et al [3]conducted a study of heat transfer coefficients and CO2 flow maps during boiling. The medium was tested for reduced pressure Pr from 0.21 to 0.87, mass velocity G from 170 kg/(m^2·s) to 570 kg/(m^2·s), and temperature from -28°C to 25°C. Nema et al. [4]studied the flow structures of R134a during condensation and proposed a new criterion for the transit of flow structures. Charnay et al. [5] studied the flow structures of R245fa during boiling at 60°C, which corresponds to a pressure of 4.6 bar for a mass velocity of 100 to 1,500 kg/(m^2·s) with an inner diameter of a 3mm round tube. Charnay et al. [6] conducted additional tests for a

https://doi.org/10.52202/069564-0037

saturation temperature of 120°C. They compared the results obtained with annular flow transition lines available in the literature. Although the flow structures more closely resembled those observed at the macroscale, the transition line was similar to that observed in minichannels. Barberi et al.[7] presented research on R134a boiling in in smooth brass tubes for various diameters form 6.2 mm to 12.6 mm for mass velocities from 25 to 500 kg/(m^2·s). El Hajal et al. [8]presented flow pattern map and flow pattern based heat transfer model for condensation inside horizontal plain tubes for CO2 for reduced pressure up to 0.8. Kim et al. [1,9] conducted research on flow maps and heat transfer during condensation of FC-72. They proposed flow patter prediction method which was development of Soliman method [10]Zhang et al. [2] further developed this correlation to predict low patterns for R170 for high saturation pressures from 1.5 to 2.5 MPa what correspond to reduce pressure up to 0.51 MPa. Revelin and Thome [11]in et al presented research of flow patterns of R134a ad R245fa for 26, 30 and 35 °C saturation temperatures inside 0.5 mm and 0.8 mm diameter glass tube. They proposed correlation for pattern prediction method. Ong and Thome [12]proposed new method for pattern flow prediction for R134a, R236fa and R245fa during flow boiling in small channels of 1.03, 2.20 and 3.04 mm diameter.

2. Methodology and laboratory equipment

A study was conducted to visualize the flow of two-phase modern refrigerant R1233zd for reduced pressure values from 0.2 to 0.6. and for mass velocity G [kg/(m^2·s)] from 180 to 445. The critical temperature of the tested refrigerant is 156.6°C, and the critical pressure is 21.4 bar. Its GWP (Global Warming Potential) is 1, and its ODP (Ozone Depleting Potential) is 0 according to the NIST database of Acree et al. (2022). A schematic of the test rig is shown in Figure 1. The prevailing pressure in the system is established through a pressurized nitrogen tank connected to a membrane hydroaccumulator. The main pump ensures that the medium is pumped through the system and overcomes the flow resistance. Behind the pump is a Coriolis mass flow meter. Next is the preheater, followed by a section for measuring heat transfer coefficients during boiling. Behind the measuring section is the visualization section, which is shown in Fig. 2. It consists of a borosilicon tube with an inner diameter of 3mm, a wall thickness of 3mm and a length of 200mm. Behind the visualization section is a condensation section with an intermediate oil system that provides constant condensation conditions. Images were taken with a Photron Fastcam Mini UX100 high-speed camera.

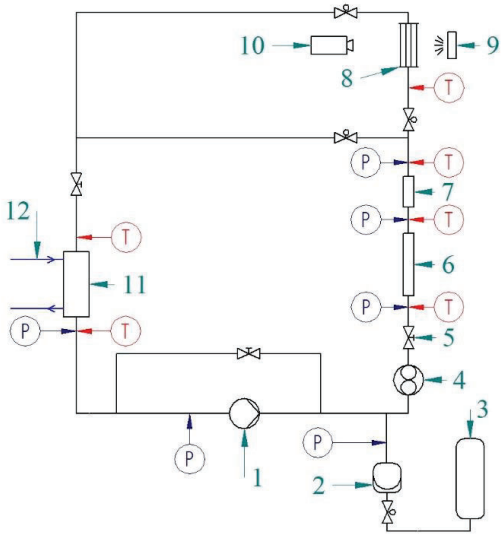

Figure 1. Test stand: 1 - piston diaphragm pump, 2 - diaphragm hydroaccumulator, 3 - pressurized nitrogen tank, 4 - Coriolis flow meter, 5 - control valve, 6 - heater, 7 - heat exchange measurement section, 8 - visualization section, 9 - led light source, 10 - high-speed camera, 11 - condenser, 12 - oil loop.

https://doi.org/10.52202/069564-0037

Figure 2. The visualization section with the Photron Fastcam Mini UX100 high-speed camera. Behind the visualization section is an led light source.

3. Flow patterns

Tests were conducted for reduced pressures Pr from 0.2 to 0.8 of the critical pressure value. The mass velocities tested were 180, 265, 355 and 445 kg/(m^2·s). Figure 3 shows the flow structures for Pr=0.2, while Figure 4 shows the flow structures for Pr=0.4, Figure 5 shows the structures for Pr=0.6, Figure 6 shows the structures for Pr=0.7 and Figure 7 show flow structures for Pr=0.8. All figures show the same mass velocity of G=355 kg/(m^2·s), which makes it possible to compare the differences in flow structures. Due to the large difference in the specific volume ratio of the liquid and gas phases at a reduced pressure of 0.2, annular flow already occurs at a dryness degree of x=7%, while for a quality of 0.8, annular flow occurs at x=45%. Bubble flow was defined as when bubbles alone are present. Slug flow was defined as when single plugs are present. When the flow is dominated by multiple plugs that are close to merging into a ring, or when the ring was not continuous the flow was defined as intermittent. In Fig. 3, one can observe the slug and annular flow. In Fig. 4 and Fig. 5, bubble, plug, intermittent and annular flows can be observed. Fig. 5, Fig. 8, Fig. 9, Fig. 10 show the flow structures for Pr=0.6 and for mass velocities of G=355 kg/(m^2·s), G=180 kg/(m^2·s), G=265 kg/(m^2·s) and G=445 kg/(m^2·s), respectively. In particular, one can observe the later appearance of ring structure for lower mass velocities. This trend is shown in the flow maps in the next section. For reduced pressures 0.7 and 0.8 bubbles can be observed even when annular follow emerged. This is unique structure which can be only observed at vicinity of thermodynamical critical point.

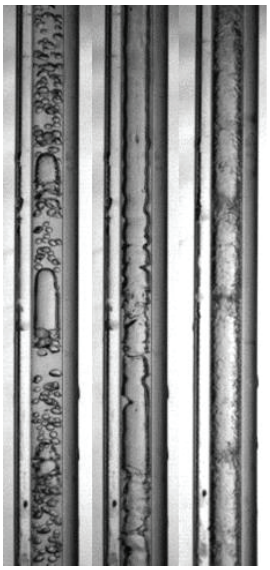

Figure 3. Flow Patterns Pr=0,2 G=355 kg/(m^2·s) Quality respectively: 2%, 7%, 5,03%

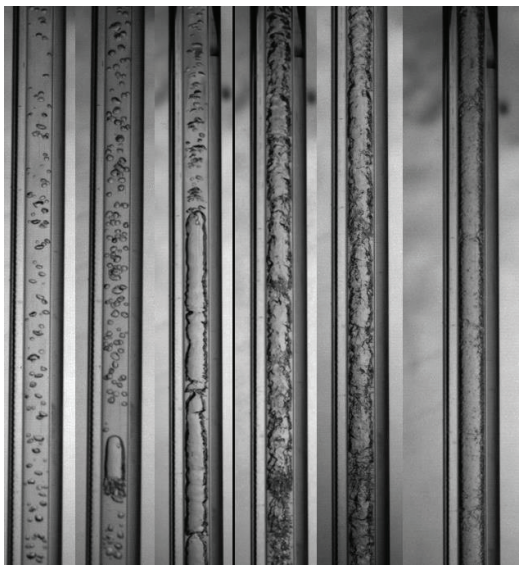

Figure 4. Flow Patterns Pr=0,4 G=355 kg/(m^2·s) Quality respectively: 3,1%, 4,2%, 10%, 23,1%, 80,5%

https://doi.org/10.52202/069564-0037

Figure 5. Flow Patterns Pr=0,6 G=355 kg/(m^2·s) Quality respectively: 12%, 15,6%, 19,6%, 23,9%, 36,2%, 60,7%

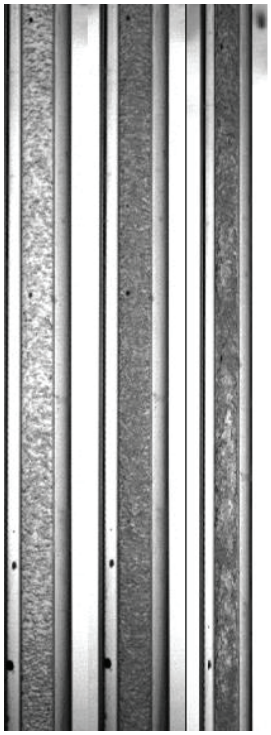

Figure 6. Flow Patterns Pr=0,7 G=355 kg/(m^2·s) Quality respectively: 8.5%, 18.6%, 46%.

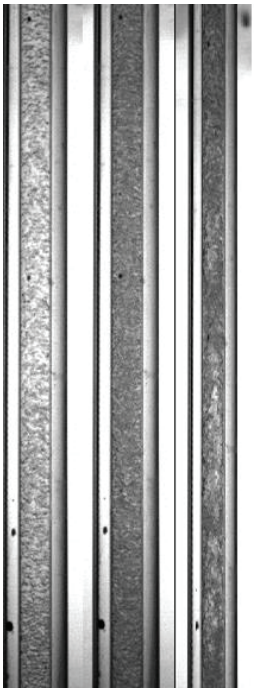

Figure 7. Flow Patterns Pr=0,8 G=355 kg/(m^2·s) Quality respectively: 8.2%, 19%, 33,7%.

Figure 8. Flow Patterns Pr=0,6 G=180 kg/(m^2·s) Quality respectively: 37,2%, 48,6%, 64,6%, 72,8%, 93%

https://doi.org/10.52202/069564-0037

Figure 9. Flow Patterns Pr=0,6 G=265 kg/(m²·s) Quality respectively: 19,6%, 27%, 35,2%, 55,6%

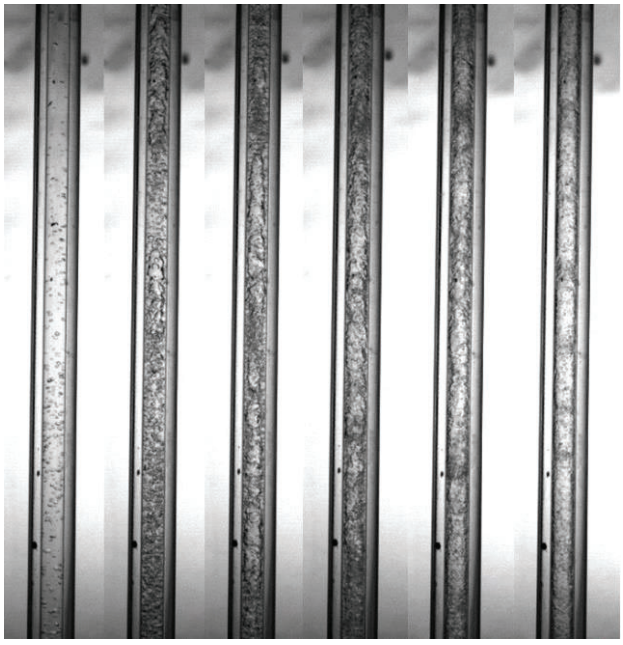

Figure 10. Flow Patterns Pr=0,6 G=445 kg/(m²·s) Quality respectively: 8,5%, 15,9%, 23,7%, 36,5%, 52,4%, 67,6%

4. Flow maps and new annular flow prediction method

In recent years flow maps were primarily presented as Mass flow in function of quality. This presentation method allow to easily compare patterns with experiment and heat transfer coefficient measurements.

4.2. New correlation to determine transition line to annular flow

A new prediction method for determination of flow pattern transition into annular flow is proposed. Its is modification of correlation proposed by Revelin et al. [13] Original correlation presented good prediction at lower values of reduced pressure 0.3 and 0.4 what can be observed in the Figures 12 and 13. Is is good result we take in into account that this method was created for different fluid and different diameter. That correlation is based on fluids R134a and R245fa at 26, 30 and 35 °C saturation temperatures inside 0.5 mm and 0.8 mm diameter glass tube. In the Figure 18 it can be observed that method proposed by Ravelin do not follow trend of annular transition line for different values of reduced pressure. In fact it showed that annular flow occurs fasters at high reduced pressure. Experimental data show opposite trend. Because of that Bond number was introduced to the equation. Bond number represents effect of gravitational forces compared to surface tension forces for the movement of liquid. When significance of surface tension value of this criterial number is higher. Surface tension decreases for higher value of saturation temperature. This change allowed to adapt transition line for all reduced pressures what can be observed in the Fig 18. Formula for transition line between intermittent flow and annular flow is:

$$x_{i/a} = Rel^{1.47}/Wel^{1.23} \cdot Bo^{1.9} \cdot 3.5 \cdot 10^{-7} \quad (1)$$

4.3. Flow maps with transition lines for R1233zd(E)

Fig. 11 shows the flow map for reduced pressure of 0.2, Fig. 12 shows the flow map for Pr=0.3, Fig. 13 shows the flow map for Pr=04, Fig. 14 shows the flow map for Pr=0.5, Fig. 15 shows the flow map for Pr=0.6 Fig. 16 shows the flow map for Pr=0.7, and Fig. 16 shows the flow map for Pr=0.6. Fig. 17 shows the flow map for mass velocity G=355 kg/(m^2*s) as a function of reduced pressure and quality. In Figures 11 through 16, an inverse correlation can be observed between mass velocity and the occurrence of annular flow. Annular flow occurs fastest for a reduced pressure of 0.2, and latest for Pr=0.8. This is a result of the smaller difference between the unit specific volume of the gas phase and the liquid phase, and the lower surface tension of the liquid phase. The delayed occurrence of annular flow also occurs for lower values of mass velocity. 7 correlations for transition of flow pattern into annular flow is presented in the flow maps for various values of reduced pressure and mass velocity. This correlations are proposed by Ong and Thome[12], Revelin and Thome [11],Cheng et al. [3], El Hajal et al. [8]Zhuang et al. [2], Kim and Mundawar [9] and last one is the one

proposed in this article. None of this correlations was created for exact conditions as in experiment conducted by authors. Correlations of El Hajal and Cheng were created for CO_2 for high values of reduced pressure up to 0.8. Zhuang proposed correlation for medium values of reduced pressure for ethane. Other correlations were created for low values of reduced pressure. Correlations proposed by Revelin and Thome and by Ong and Thome showed good results for Pr around0.3 and 0.4. Method proposed by Kim and Mundawar was second best correlation and predicted flow correctly from 0.2 up to 0.5 value of reduced pressure. All correlations expressed correct trend between mass velocity and transition line except from Correlations proposed by El Hajal and Cheng. New correlation correctly predict trends for various value of reduced pressure and various mass velocities.

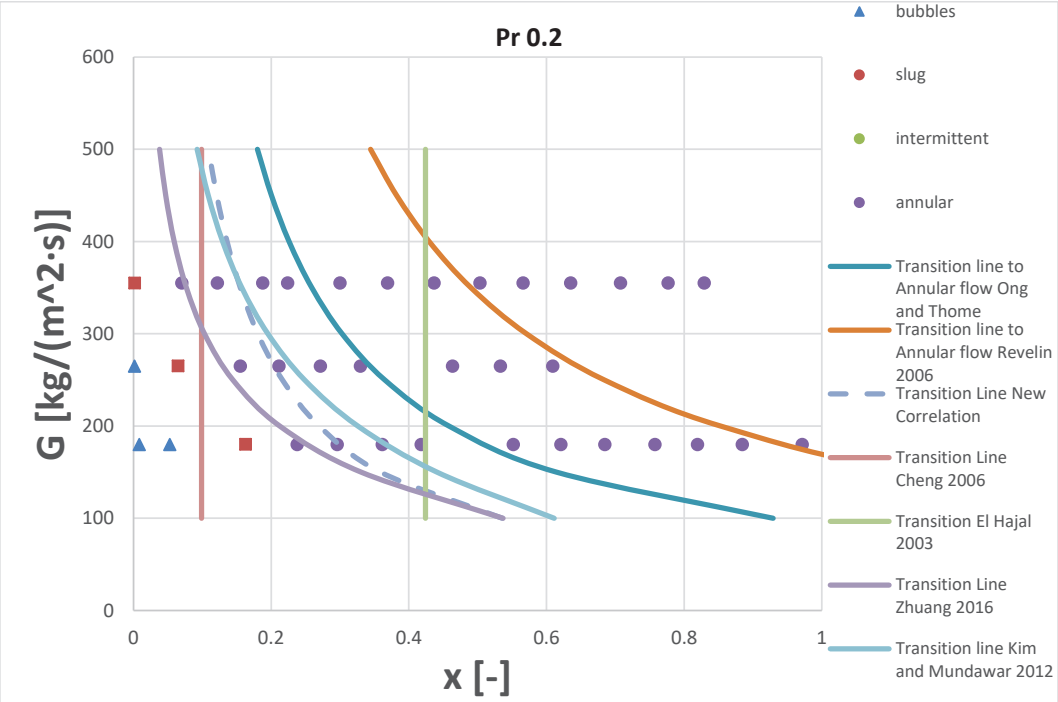

Figure. 11. Flow map for reduced pressure 0.2

https://doi.org/10.52202/069564-0037

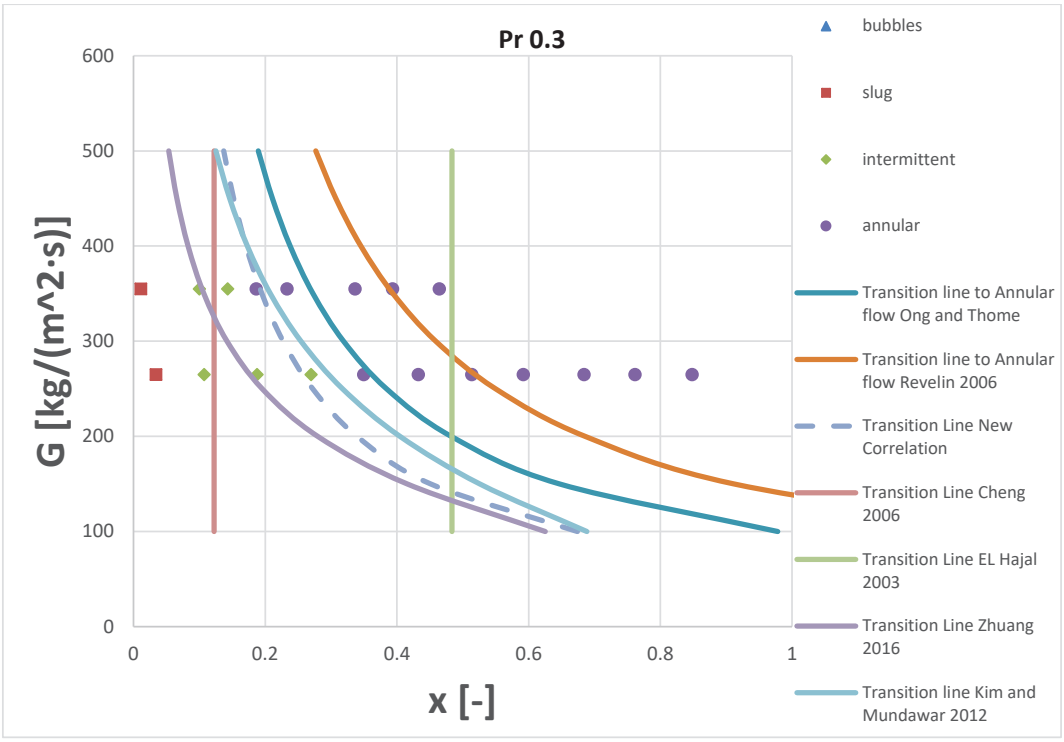

Figure. 12. Flow map for reduced pressure 0.3

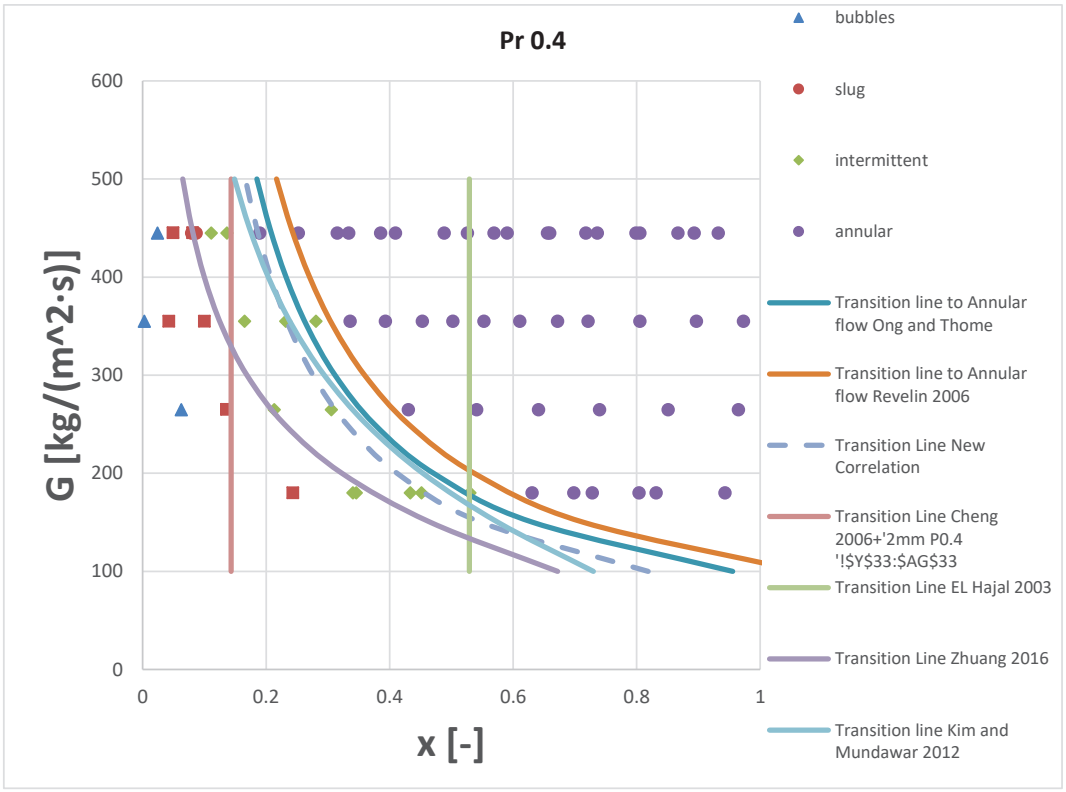

Figure. 13. Flow map for reduced pressure 0.4

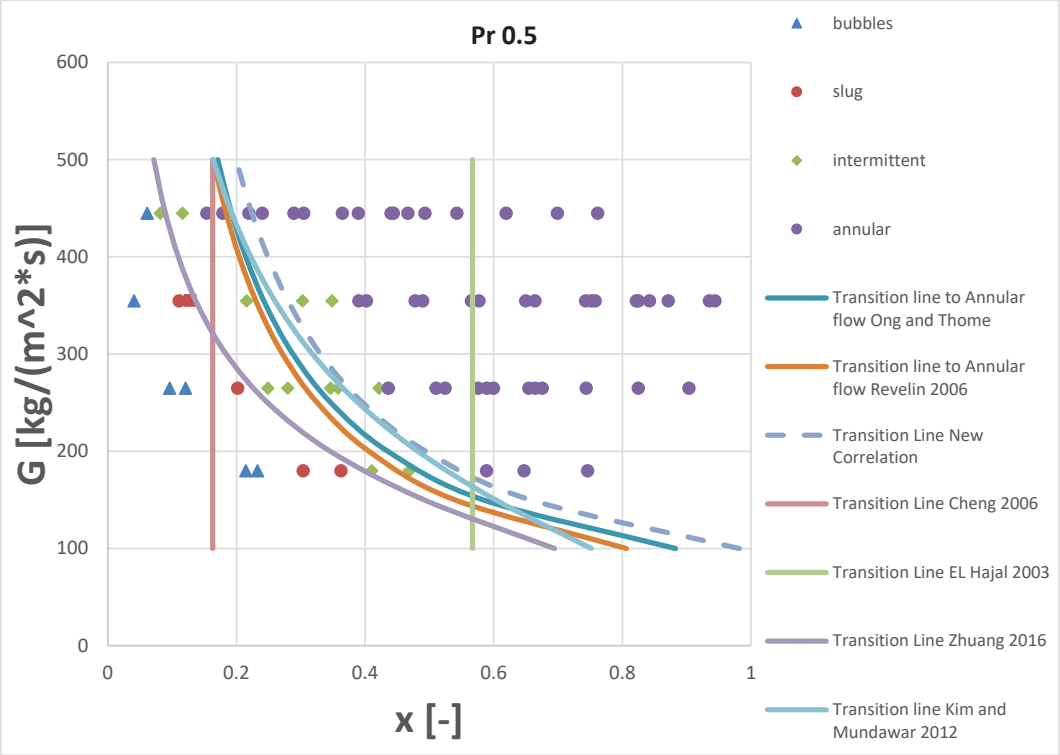

Figure. 14. Flow map for reduced pressure 0.5

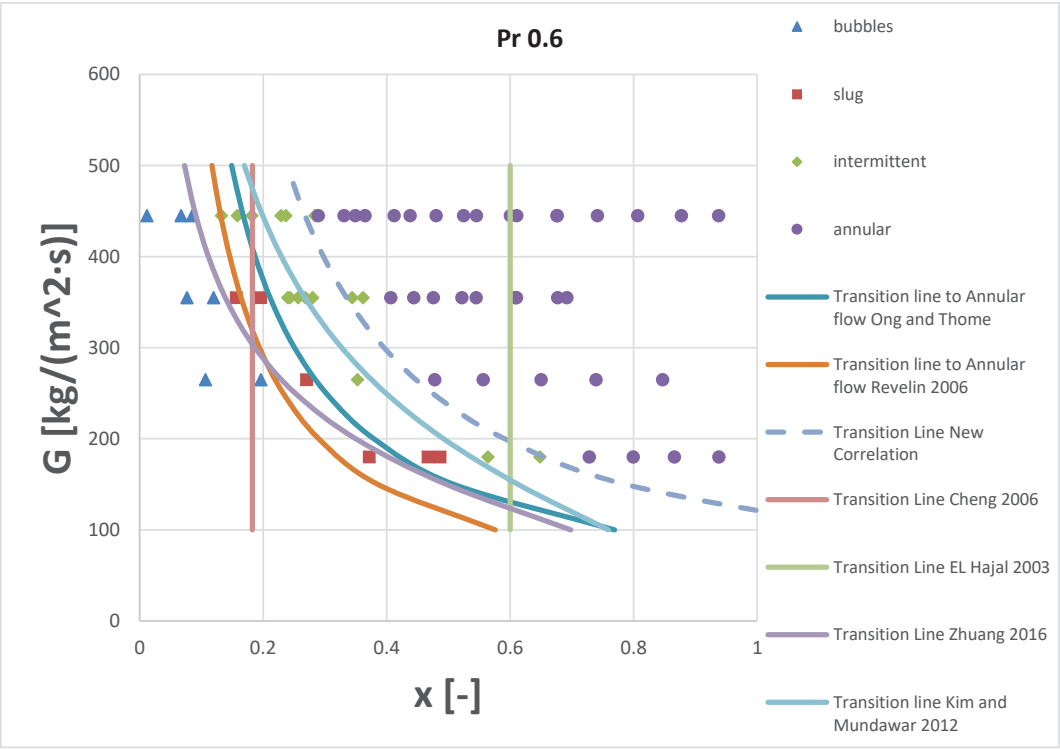

Figure. 15. Flow map for reduced pressure 0.6

https://doi.org/10.52202/069564-0037

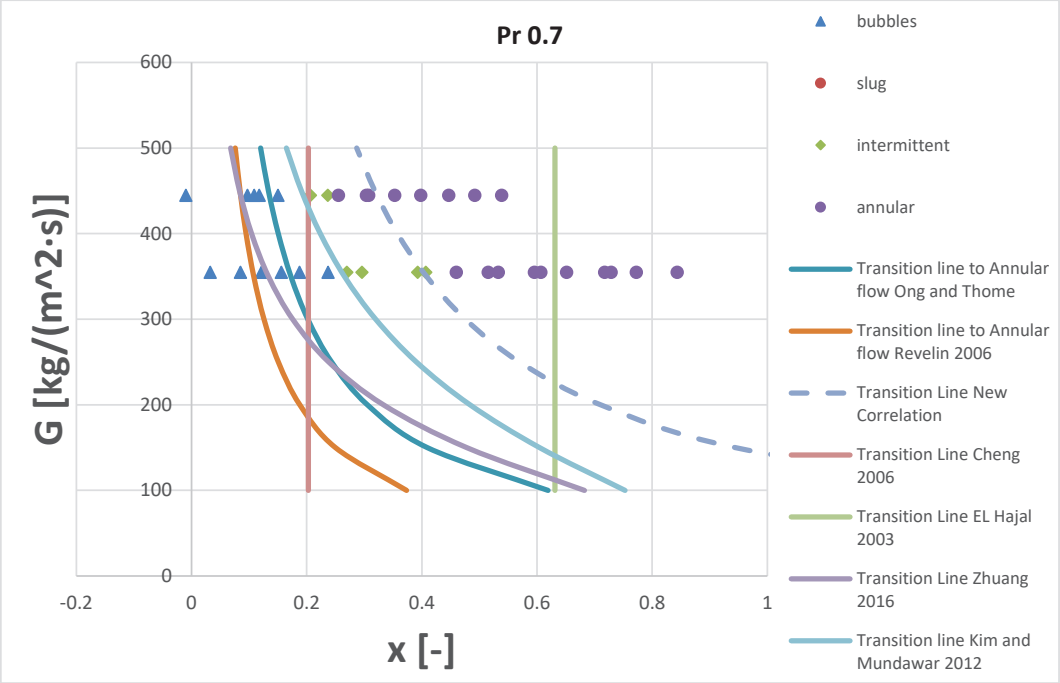

Figure. 16. Flow map for reduced pressure 0.7

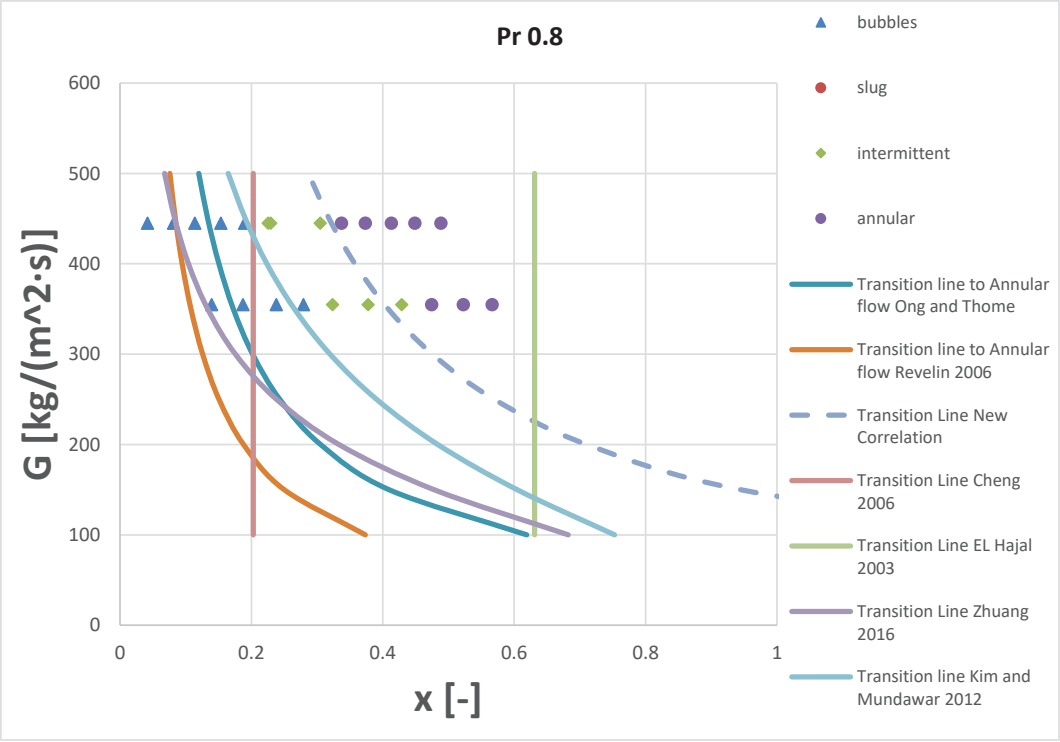

Figure. 17. Flow map for reduced pressure 0.8

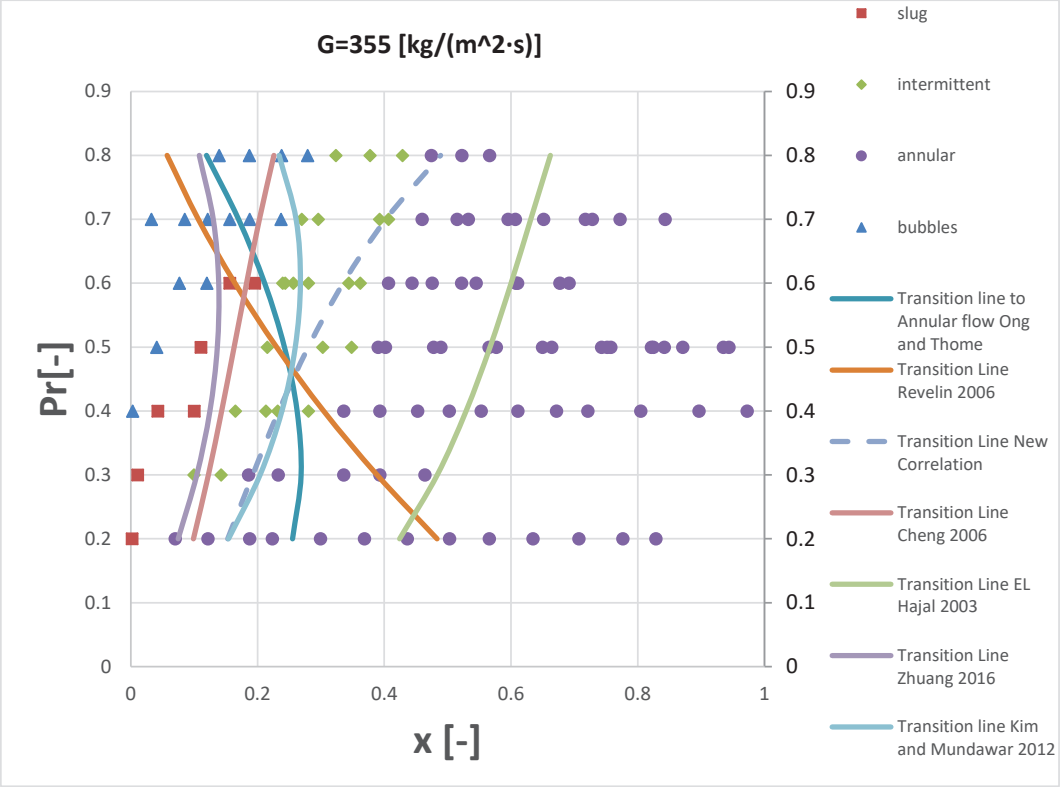

Figure. 18. Flow map for reduced pressure ranging from 0.2 to 0.8 for mass flow 355 [kg/(m^2*s)]

Table 1. Comparison of correlations which predict annular flow for collected database for R1233zd(e).

Correlation	number of experimental data points correctly calculated	percentage of experimental data points correctly calculated
Ong and Thome [12]	238	78.81%
Revelin et al. [11]	214	70.86%
New corelation	276	91.39%
Cheng et al. [3]	236	78.15%
El Hajal et al. [8]	215	71.19%
Zhuang et al. [2]	227	75.17%
Kim and Mundawar [1]	262	86.75%

Comparison of all tested correlations is presented in Table 1. Authors correlation managed to correctly predict 91,39% of collected experimental data points. Second best is correlation presented by Kim and Munawar [1] which predicted 86.75% points. Other correlations managed to predict from 70% to 75% of data point despite not being able to follow experimental transition lines.

4.3. Applicability of new correlation for different fluids.

Applicability of new correlation for different fluids was tested on data collected by Charnay et al.[5,6]. Authors correlation follow experimental transition trend also for this fluid. Experimental lines for all correlations are presented in the Fig 19. Data is presented as function of Reduced pressure and quality

https://doi.org/10.52202/069564-0037

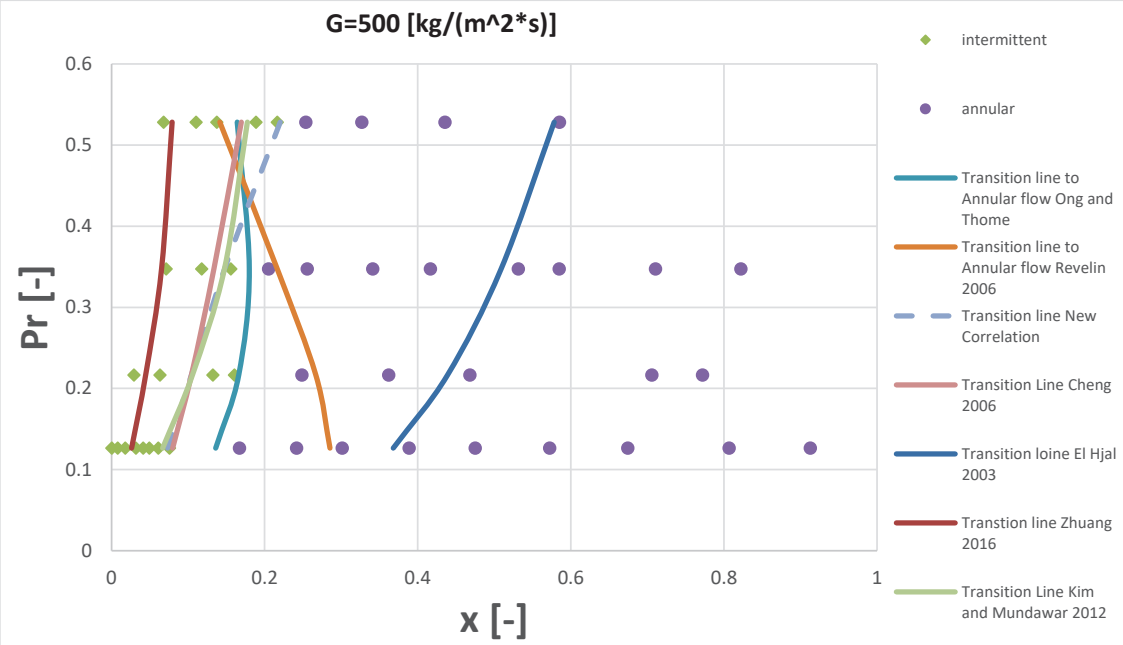

Figure. 19. Flow map for reduced pressure ranging from 0.13 to 0.53 for mass flow 500 [kg/(m^2*s)] for R245fa collected by Charnay et al. [5,6]

5. Conclusions

The change in the physical properties of refrigerants as the saturation temperature increases has a major impact on structures and flow maps. At high values of reduced pressure, the density of the gas phase is relatively high, and the density of the liquid phase is low. There is a low specific volume difference between the liquid and gas phases. These properties cause a delay in the occurrence of annular flow. For reduced pressure 0.8 annular flow occurred at 45% of quality for G=355 [kg/(m^2*s)] and for reduced pressure 0.2 it was visible at 7% of quality. Since the presence of bubbles in the flow occurs for much higher quality at higher reduced pressures nucleation as a heat transfer mechanism is more important for boiling at high saturation temperatures. It is also worth noting the delayed occurrence of annular flow for lower values of mass velocity. Further work should focus on expanding the experimental database. Old correlations for annular transitions lines prediction did not manage correctly to predict transition of flow pattern to annular flow for high reduced pressures. Most of them predicted trend opposite to measured for increasing saturation pressure. They predicted that annular flow occurs faster for high values of reduced pressure, but in fact annular flow occurs later for high saturation pressure. New correlation for annular flow transition line is able to predict transition form intermittent flow into annular flow for all measured reduced pressures and mass velocities. Authors correlation managed to correctly predict 91,39% of collected experimental data points what is best results of all tested correlations.

Nomenclature

Bo Bond, -

G mass velocity, kg/(m^2*s)

Pr reduced pressure -ratio of pressure to critical pressure, -

Rel Reynolds number for saturated liquid $Rel = \frac{GD}{\mu l}$, -

Rev Reynolds number for saturated vapour $Rev = \frac{GD}{\mu v}$, -

t temperature, °C

Wel Weber number for saturated liquid $Wel = \frac{G^2 D}{\rho l}$, -

x Quality, -

https://doi.org/10.52202/069564-0037

Acknowledgements

This research was funded in whole or in part by National Science Centre, Poland 2017/25/B/ST8/00755
This research was funded in whole or in part by National Science Centre, Poland 2021/41/N/ST8/04421

References

[1] Kim S.M., Mudawar I., Flow Condensation in Parallel Micro-Channels - Part 2: Heat Transfer Results and Correlation Technique. International Journal of Heat and Mass Transfer 2012;55:984–994.

[2] Zhuang X., Gong M., Chen G., Zou X., Shen J., Two-Phase Flow Pattern Map for R170 in a Horizontal Smooth Tube. International Journal of Heat and Mass Transfer 2016;102:1141–1149.

[3] Cheng L., Ribatski G., Wojtan L., Thome J.R., New Flow Boiling Heat Transfer Model and Flow Pattern Map for Carbon Dioxide Evaporating inside Horizontal Tubes. International Journal of Heat and Mass Transfer 2006;49:4082–4094.

[4] Nema G., Garimella S., Fronk B.M., Flow Regime Transitions during Condensation in Microchannels. International Journal of Refrigeration 2014;40:227–240.

[5] Charnay R., Revellin R., Bonjour J., Flow Pattern Characterization for R-245fa in Minichannels: Optical Measurement Technique and Experimental Results. International Journal of Multiphase Flow 2013;57:169–181.

[6] Charnay R., Bonjour J., Revellin R., Experimental Investigation of R-245fa Flow Boiling in Minichannels at High Saturation Temperatures: Flow Patterns and Flow Pattern Maps. International Journal of Heat and Fluid Flow 2014;46:1–16.

[7] Barbieri P.E.L., Jabardo J.M.S., Bandarra Filho E.P., Flow Patterns in Convective Boiling of Refrigerant R-134a in Smooth Tubes of Several Diameters. European Thermal-Sciences Conference 2008;9.

[8] El Hajal J., Thome J.R., Cavallini A., Condensation in Horizontal Tubes, Part 1: Two-Phase Flow Pattern Map. International Journal of Heat and Mass Transfer 2003;46:3349–3363.

[9] Kim S.M., Kim J., Mudawar I., Flow Condensation in Parallel Micro-Channels - Part 1: Experimental Results and Assessment of Pressure Drop Correlations. International Journal of Heat and Mass Transfer 2012;55:971–983.

[10] Soliman H.M., On the Annular-to-wavy Flow Pattern Transition during Condensation inside Horizontal Tubes. The Canadian Journal of Chemical Engineering 1982;60:475–481.

[11] Revellin R., Thome J.R., Experimental Investigation of R-134a and R-245fa Two-Phase Flow in Microchannels for Different Flow Conditions. International Journal of Heat and Fluid Flow 2007;28:63–71.

[12] Ong C.L., Thome J.R., Macro-to-Microchannel Transition in Two-Phase Flow: Part 1 - Two-Phase Flow Patterns and Film Thickness Measurements. Experimental Thermal and Fluid Science 2011;35:37–47.

[13] Revellin R., Dupont V., Ursenbacher T., Thome J.R., Zun I., Characterization of Diabatic Two-Phase Flows in Microchannels: Flow Parameter Results for R-134a in a 0.5 Mm Channel. International Journal of Multiphase Flow 2006;32:755–774.

https://doi.org/10.52202/069564-0037